

Electronic Supplementary Information

Protein Corona Meets Freeze-Drying: Overcoming the Challenges of Colloidal Stability, Toxicity and Opsonin Adsorption

Agustín S. Picco,^{1,2#} Gabriela Borba Mondo,^{1,3#} Larissa F. Ferreira,^{1,4} Edmarcia E. de Souza,¹ Luís A. Peroni,⁵ Mateus Borba Cardoso^{1,3,4}*

¹ Brazilian Synchrotron (LNLS) and Brazilian Nanotechnology Laboratory (LNNano), Brazilian Center for Research in Energy and Materials (CNPEM), Zip Code 13083-970, Campinas, Brazil.

² Instituto de Investigaciones Fisicoquímicas Teóricas y Aplicadas (INIFTA), Fac. de Cs. Exactas, Universidad Nacional de La Plata - CONICET, Diagonal 113 y 64, Zip Code 1900, La Plata, Argentina

³ Institute of Chemistry (IQ), University of Campinas (UNICAMP), P.O. Box 6154, Zip Code 13083-970, Campinas, Brazil

⁴ Programa de Pós-Graduação em Biotecnociência, Universidade Federal do ABC, Zip Code 09210-580, Santo André, Brasil.

⁵ Brazilian Biosciences National Laboratory (LNBio), Brazilian Center for Research in Energy and Materials (CNPEM), Zip Code 13083-970, Campinas, Brazil

Equal contribution

* cardosomb@lnls.br

TABLE OF CONTENTS

Section S1: STEM, SEM, SAXS and DLS characterizations of SNPs

Section S2: Hemolytic activity assay

Section S3: Cytotoxicity assay

Section S4: Live cell confocal microscopy procedure

Section S5: Bovine γ -globulin adsorption experiments

Section S6: Evolution of SNP-FD_{BSA1%} size after resuspension / Impact of storage on SNP-FD_{BSA1%}

Section S7: STEM of SNP-FD_{BSA1%} after freeze-drying

Section S8: Evaluation of Dh_2/Dh_1 for SNP freeze-dried in presence of increasing concentrations of BSA

Section S9: TGA of SNP after incubation with different BSA concentrations

Section S10: Theoretical estimation of the mass fraction corresponding to a BSA monolayer

Section S11: TGA of SNP-FD_{BSA1%} after freeze-drying and washing

Section S12: Brief exploration on the freeze-drying of SNPs with different sizes

Section S13: Raw optical density data from hemolytic activity assay

Section S14: Brief exploration on the use of other proteins than BSA as protectants for the freeze-drying of SNPs

Section S15: Impact of washing on the DLS-based size of SNPs incubated with 1% w/v BSA

Section S16: Brief evaluation on freeze-drying of SNP with freezing step carried at higher temperature

Section S17: Impact of sonication in SNP-FD

Section S18: References

Section S1: STEM, SEM, SAXS and DLS characterization of SNPs

STEM images were acquired using a SEM-FEG FEI Inspect F50 microscope which was operated at 30 kV (bright-field acquisition mode). Drop casting was used to deposit the sample on a holey carbon-coated copper grid. Size distribution was obtained by counting at least 250 nanoparticles using ImageJ software.¹

SEM images were obtained with a high-resolution Thermo Scientific Quanta 650FEG instrument (SEM-FEG). Samples were prepared by directly adding a drop of nanoparticle suspension over a copper substrate and allowing it to dry. Then, the samples were sputter-coated with Au using a Bal-Tec SCD050 Sputter Coater. Secondary back-scattered electrons were collected from Au-coated samples impinged by a 5 kV electron beam. Size distribution was obtained by counting at least 300 nanoparticles using ImageJ software.¹

SAXS characterization was performed using the SAXS1 beamline of the Brazilian Synchrotron Light Laboratory (LNLS, Campinas, Brazil; SAXS proposal 20170969). SNPs suspensions in water (at 0.2 g·L⁻¹) were used. During the measurements the sample-to-detector distance was 3 m and the X-ray wavelength was set to 0.1488 nm. Sample temperature was kept using a circulating water bath. Two parallel micas were used as windows defining a 1 mm optical path sample chamber. Each pattern was corrected for beam attenuation and time integrated photon flux following regular beamline procedures. The corresponding solvent scattering was subtracted from each corrected image before analysis.

Figure S1 shows the STEM, SEM and SAXS characterization performed for the main silica nanoparticles (SNPs) used along this work. The STEM size distribution was adjusted using a log-normal distribution, obtaining $D_{STEM} = 89.0$ nm and $\sigma(\%) = 10.2\%$. The SAXS pattern was fitted using a sphere model² with a log-normal distribution accounting for the polydispersity, as implemented in Sasfit Software,³ obtaining $D_{SAXS} = 91.5$ and $\sigma(\%) = 9.9\%$. The SEM size distribution was adjusted using a log-normal distribution, obtaining $D_{SEM} = 103.6$ nm and $\sigma(\%) = 9.0\%$. The bigger sizes observed by SEM can be attributed to the gold coating deposited over the nanoparticles.

DLS was used to evaluate nanoparticle size (as hydrodynamic diameter, D_h), size distribution and aggregation in the resuspended powders. The measurements were carried out using a Malvern Zetasizer ZS, equipped with a red laser ($\lambda = 632.8$ nm) and operated in backscattering mode (detection angle = 173°). Measurements were performed in triplicates, each one consisting of 10 runs of 10 seconds, at the desired temperature with a thermal stabilization period of 120 seconds. The correlation curves were analyzed using Cumulant Analysis to obtain Z-Average hydrodynamic diameters, and a Non-Negative Least Square (NNLS) fitting algorithm (General Purpose) to extract size distributions,⁴ both of them implemented in the Malvern Zetasizer Software.

The dynamic viscosity (μ) and refractive index (n) of the different media used were estimated to properly calculate hydrodynamic diameters. μ and n of the solutions with different concentrations of BSA in water and PBS were estimated using the values provided by the DLS equipment data base ($\mu_{water} = 0.8872$ cP and $n_{water} = 1.330$; $\mu_{PBS} = 0.8882$ cP and $n_{PBS} = 1.330$; both at 25°C) and BSA's intrinsic viscosity^{5,6} and differential refractive index.⁷ For complex media (e.g. DMEM supplemented with 10% v/v FBS plus the BSA coming from the freeze-dried powder), μ was determined using a

Cannon-Fenske 25 tube viscometer and an Anton Paar density meter DMA 4500, while n using a Brookhaven BI-DNDC differential refractometer ($\lambda = 620$ nm) using ultrapure water as reference. Table S1 presents the obtained values for different media.

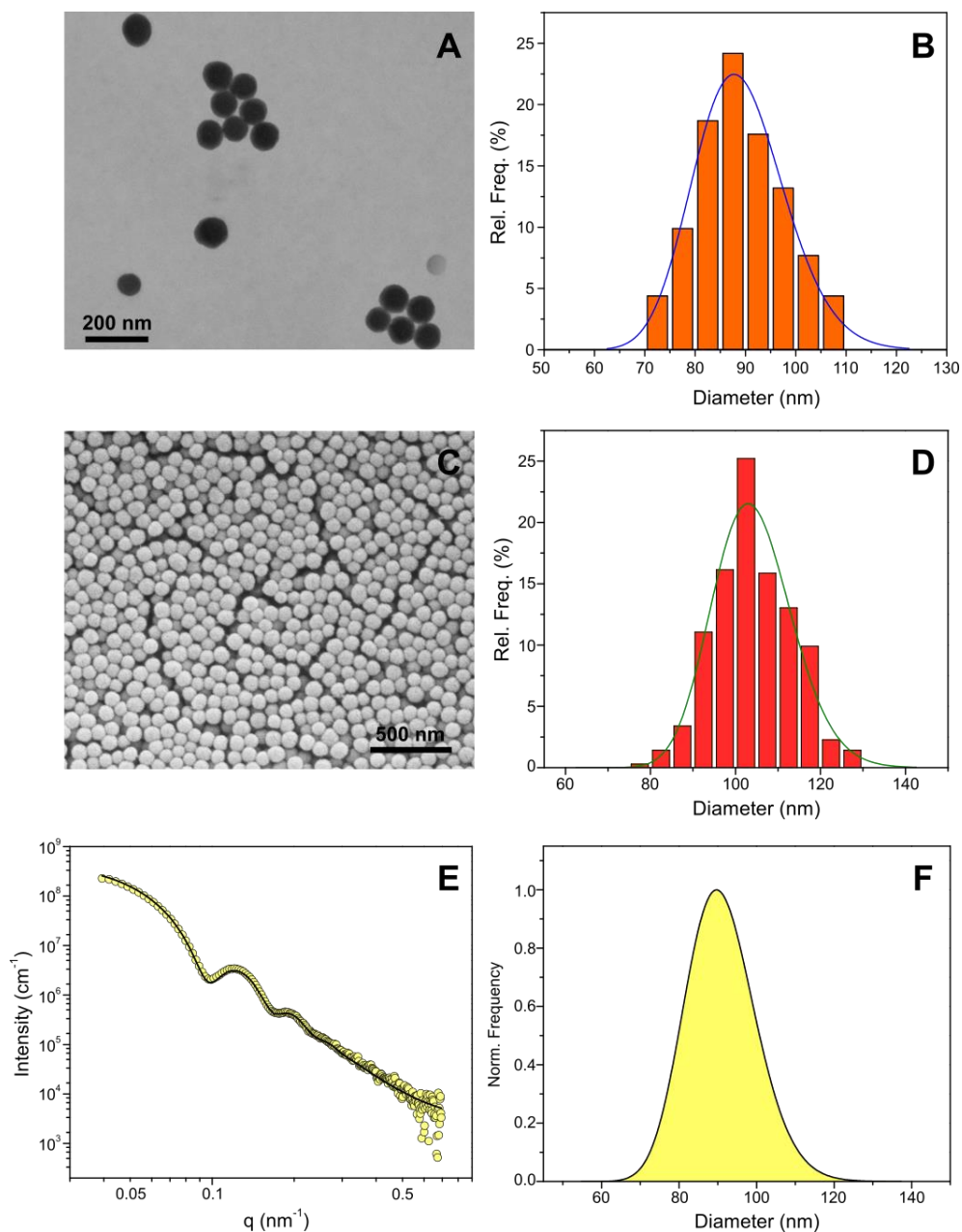


Figure S1. (A) Representative STEM micrography of SNP. (B) STEM-based size distribution obtained for SNP. (C) Representative SEM micrography of SNP. (D) SEM-based size distribution obtained for SNP (E) SAXS pattern of SNP in water at $0.2 \text{ g}\cdot\text{L}^{-1}$. The solid black line represents the best fit using a polydisperse sphere model. (F) SAXS-based size distribution.

TABLE S1. Refractive index and Dynamic viscosities of selected media at 37°C

Media	Refractive Index	Dynamic viscosity (cP)*
DMEM	1.3326	0.7118
s-DMEM	1.3333	0.7189*
s-DMEM + 1% BSA	1.3340	0.7477*
RPMI	1.3319	0.7047
s-RPMI	1.3327	0.7129*
s-RPMI + 1% BSA	1.3341	0.7432*

* Dynamic viscosity DMEM and RPMI supplemented with FBS and FBS + BSA (1%w/v) where calculated using the density values obtained for the pure cell culture media

Section S2: Hemolytic activity assay

Human red blood cells (RBCs, type O+), stored in plastic bags of transfusion service, were kindly provided by the Hemocenter from the Faculty of Medicine - University of Campinas (UNICAMP, Campinas, São Paulo, Brazil). Before incubation with the nanoparticles, the RBCs were washed 3 times with PBS solution. Shortly, 5 mL of RBCs concentrate were diluted with 35 mL of PBS solution, centrifuged at 5000 rpm for 10 min at 4 °C (Eppendorf centrifuge 5810 R) and the supernatant discarded. A stock RBC suspension (10%) in PBS was prepared by adding 9 mL of PBS solution to 1 mL of purified RBCs concentrate, and was used in all hemolytic assays.

All investigated samples were dispersed in PBS solution in sterile microtubes at room temperature immediately before RBC incubation. 0.1 mL of the RBC stock-suspension was added to 0.9 mL of sample solutions in PBS, and incubated for 60 min at room temperature (22 ± 1 °C) under gentle shaking after homogenization. SNP concentrations were calculated considering the final volume of 1.0 mL.

Positive (PC, 100% hemolysis) and negative (NC, 0% hemolysis) controls were prepared by incubating RBC with deionized water and PBS solution, respectively, with equivalent BSA concentrations when pertinent.

For dose-response curves, sample suspensions were prepared by diluting the resuspended SNP-FD in PBS at different concentrations. The positive (PC, 100% hemolysis) and negative (NC, 0% hemolysis) controls were prepared by incubating RBC with deionized water and PBS solution, respectively. In order to estimate the nanoparticle concentration resulting in 50% of hemolysis (HD_{50}) a four-parameter logistic curve was fit.

Freeze-dried powders $SNP-FD_{BSA1\%}$, $SNP-FD_{BSA0,6\%}$, $SNP-FD_{BSA0,2\%}$ were resuspended in PBS and diluted at selected nanoparticle concentrations for RBC incubation to evaluate the effect of the BSA on the hemolytic activity of lyophilized SNPs. BSA solutions at equivalent concentrations were prepared in deionized water and PBS and used as positive and negative controls, respectively.

After incubation, the tubes were centrifuged at 10000 rpm for 10 min at 4 °C, and 0.2 mL aliquots of supernatant were transferred to a clean 96-well plate. Absorbance of released hemoglobin was measured at 540 nm with a microplate reader (Thermo Multiskan GO). Hemolysis percentages were calculated using the following formula:

$$\% \text{ hemolysis} = \left(\frac{\text{Sample Absorbance} - \text{NC Absorbance}}{\text{PC Absorbance} - \text{NC Absorbance}} \right) \times 100$$

The hemolytic assay in all experiments was performed in triplicates.

Section S3: Cytotoxicity assay

Cytotoxicity of SNP-FD and SNP-FD_{BSA1%} was evaluated on the human lung adenocarcinoma A549 cells using the resazurin-based alamarBlue™ cell viability assay (Thermo Fisher Scientific).

Prior to nanoparticle incubation, SNP-FD and SNP-FD_{BSA1%} were resuspended at $1\text{g}\cdot\text{L}^{-1}$ using RPMI 1640 medium supplemented with 10% FBS (s-RPMI) and diluted in this medium to reach the desired concentrations. A549 cells were diluted in s-RPMI and plated in 96-well microplates at a density of 10 000 cells per well. Then, cells were incubated for 24 h at 37 °C in 5% CO₂ atmosphere to reach approximately 70% confluence.

These tests were performed in a laboratory facility regularly tested for endotoxin contamination. In addition, microbiological contamination of SNPs seemed to be negligible since during the resuspension tests in cell culture media (supplemented and non-supplemented with FBS) there was no observable changes in appearance of the redispersions during long times (even 2 weeks). Moreover, as shown below (section S6 figure S3 B), the size distribution of SNP-FD_{BSA1%} redispersed in cell culture media (with FBS) remains almost unaltered for at least 72h. In such conditions, pretty noticeable changes in the DLS are observed (owing to microbial growth) when microbial contamination is present.

The FBS used in these assays was purchased from Gibco (Cat. Num. 12657, Lot Num. 210420K). The certificate of analysis informs values for total protein, albumin, alpha globulin, beta globulin and gamma globulin concentrations (all converted to g/L) of 49.3, 27.2, 19.1, 3.0, $\sim 0.12\text{g}\cdot\text{L}^{-1}$, respectively.

Under this condition, the culture medium was replaced by the culture medium containing 0.05, 0.2, 0.5 and $1.0\text{g}\cdot\text{L}^{-1}$ of SNP-FD or SNP-FD_{BSA1%}, and cells were incubated for another 24 h, then washed three times with PBS solution. Afterward, 1X alamarBlue reagent prepared in RPMI 1640 without FBS (RPMI) was added to the cells, and then incubated for 1-4 h at 37 °C and 5 % CO₂ atmosphere in the dark. Immediately, the supernatant (100 μL) was transferred to a microplate reader and fluorescence emission of the formed resorufin dye was determined employing a PerkinElmer EnSpire Multimode Plate Reader using 560 nm and 590 nm as excitation and emission wavelengths, respectively.

Non-treated cells were used as positive control (PC, 100% of viability) while negative control (NC, 0% of viability) consisted of s-RPMI without cells. Moreover, another control containing s-RPMI + 1% w/v of BSA was run in parallel to discard any detrimental effect due to the excess of BSA. No significant differences were observed compared to PC.

The calculated total protein (TotP) and albumin (BSA) media concentrations in each tested condition were the following (based on FBS and freeze-dried powders contributions): NC, PC and all SNP-FD (TotP $\sim 4.9\text{g}\cdot\text{L}^{-1}$, BSA $\sim 2.7\text{g}\cdot\text{L}^{-1}$); PC supplemented with 1% wt. BSA (TotP $\sim 14.9\text{g}\cdot\text{L}^{-1}$, BSA $\sim 12.7\text{g}\cdot\text{L}^{-1}$); SNP-FD_{BSA1%} at $0.05\text{g}\cdot\text{L}^{-1}$ (TotP $\sim 5.4\text{g}\cdot\text{L}^{-1}$, BSA $\sim 3.2\text{g}\cdot\text{L}^{-1}$); SNP-FD_{BSA1%} at $0.2\text{g}\cdot\text{L}^{-1}$ (TotP $\sim 6.9\text{g}\cdot\text{L}^{-1}$, BSA $4.7\text{g}\cdot\text{L}^{-1}$); SNP-FD_{BSA1%} at $0.5\text{g}\cdot\text{L}^{-1}$ (TotP $\sim 9.9\text{g}\cdot\text{L}^{-1}$, BSA $\sim 7.7\text{g}\cdot\text{L}^{-1}$); SNP-FD_{BSA1%} at $1.0\text{g}\cdot\text{L}^{-1}$ (TotP $\sim 14.9\text{g}\cdot\text{L}^{-1}$, BSA $12.7\sim\text{g}\cdot\text{L}^{-1}$).

All tests were run in quadruplicates and the cell viability percentage was calculated using the following equation:

$$\% Viability = \left(\frac{Sample\ fluorescence - NC\ fluorescence}{PC\ fluorescence - NC\ fluorescence} \right) \times 100$$

Section S4: Live cell confocal microscopy procedure

A549 cells were seeded in a cell culture dish with glass bottom, 4 chambers well, at a density of 20 000 cells per well in growth medium (s-RPMI) and incubated for 24 h at 37°C and 5% CO₂ atmosphere. Next, cells at about 70% confluence were stained with 100 nM MitoTracker®, a mitochondria marker, diluted in incomplete RPMI 1640 medium, following 15 min incubation and three washing steps with PBS solution. Subsequently, the cells were treated with SNP-FD or SNP-FD_{BSA1%} diluted in growth RPMI 1640 medium to a final concentration of 0.2 g·L⁻¹ and incubated for 24 hours. Cells without nanoparticle addition were used as a control.

From the glass bottom dish, a series of Z stack images of interphase cells were captured from 0.35 µm thick sections using a Confocal Laser Scanning Microscope (SP8, Leica Microsystems), equipped with a 63x water - immersion objective lens. The cells were maintained in a constant environmental at 37 °C and fields of interests were acquired at randomly selected areas during live-cell imaging acquisition. At least 60 cells were imaged for each treatment from two independent experiments. Images were analyzed using ImageJ software.¹

Section S5: Bovine γ -globulin adsorption experiments

The BGG adsorption evaluation over freeze-dried SNP-FD, SNP-FD_{BSA0.2%}, SNP-FD_{BSA0.6%}, SNP-FD_{BSA1.0%} was performed in PBS at 1 g·L⁻¹ of nanoparticles and 1% w/v of BGG. The selected freeze-dried powders were resuspended in PBS using a half of the final volume, leading to a SNP concentration of 2 g·L⁻¹.

The resuspension was done as explained before (inversion and gentle mixing in shaker for 5 min). Then, a solution of BGG at 2% w/v in PBS was added to the previously resuspended nanoparticle to reach the final volume and the desired concentrations. This mixture was incubated at 37 °C in a shaker for 4 hours.

After incubation, the nanoparticles were washed (6 times) through cycles of centrifugation (20000 g, 10 min, 4 °C) and resuspension (vortex) in order to remove non-adsorbed BGG. Once the last resuspension step was done, the nanoparticles were centrifuged again, the supernatants discarded, and the sediments resuspended in approximately one tenth of the originally centrifuged volume.

The sediment containing the nanoparticles was treated with Laemmli buffer at 95 °C for 5 min to detach and denature BGG, or any protein, from nanoparticle surface (if present). Denatured samples were loaded onto 5 - 12% polyacrilamide gel and subjected to SDS-PAGE in running buffer (25mM Trisma base, 192 mM glycine and 0.1% SDS, all from Sigma-Aldrich, USA) in a Mini-Protean Tetra Cell System (Bio-Rad, USA), according to the manufacturer's instructions. Precision Plus Protein WesternC Protein Standards (Bio-Rad, USA) were loaded in each gel. Further, proteins were transferred to a polyvinylidene difluoride (PVDF) membrane (Amersham, GE Healthcare, USA) in a Trans-Blot Turbo Transfer System (Bio-Rad, USA) at 25 V and 1.3 A for 9 min. Western blots were probed for bovine IgG and all steps were carried out at room temperature, with gentle shaking. After protein transfer, membrane was incubated with blocking buffer (5% non-fat powder milk in tris-buffer saline, Sigma-Aldrich, USA) for 60 min and washed three times with PBS + 0.1% Tween detergent (Fisher Scientific, USA). In addition, membrane was incubated for 1 h with horseradish peroxidase (HRP)-conjugated rabbit anti-bovine IgG diluted 1:10,000 (Sigma-Aldrich Inc., USA) in blocking buffer. After washing, immunoblot was developed by the enzyme chemiluminescence (ECL) method according to the manufacturer's instructions (GE Healthcare, USA).

Figure S2 shows the western blot images from two different adsorption experiments, performed in different days, following the procedure explained above. The results shown in the main text were taken from the first image.

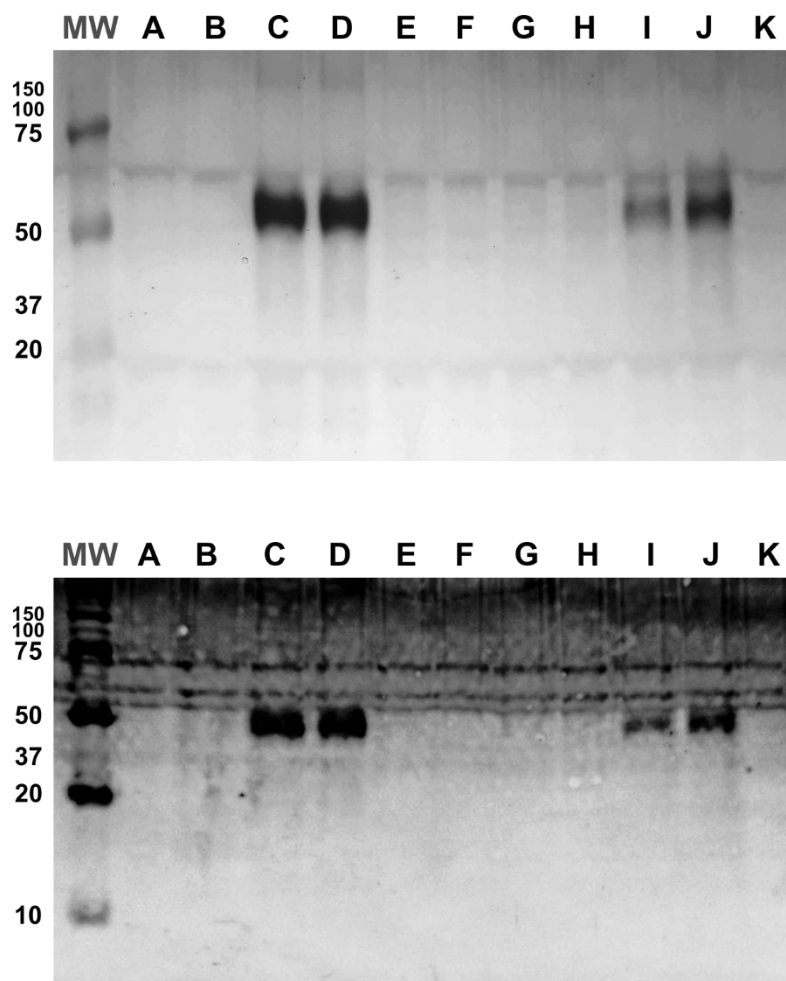


Figure S2. Western blots (full images) obtained from two different BGG adsorption experiments. Lanes: A) Free; B) BSA; C) BGG; D) BGG; E) SNP-FD_{BSA1%} after incubation with BGG; F) SNP-FD_{BSA1%} after incubation with BGG; G) SNP-FD_{BSA0.6%} after incubation with BGG; H) SNP-FD_{BSA0.2%} after incubation with BGG; I) SNP-non FD after incubation with BGG; J) SNP-FD after incubation with BGG; K) SNP-FD (control, non-incubated with BGG).

SECTION S6: Evolution of SNP-FD_{BSA1%} size after resuspension / Impact of storage on SNP-FD_{BSA1%}

The temporal evolution of SNP size distribution after being resuspended in PBS and DMEM supplemented with 10% FBS was studied for SNP-FD_{BSA1%}. Samples were resuspended by gently mixing and left at rest (static condition) until measurement. Results are shown in Figure S3. Negligible changes on the DLS-based size distribution are observed for SNP-FD_{BSA1%} after 72 h of being resuspended in both media.

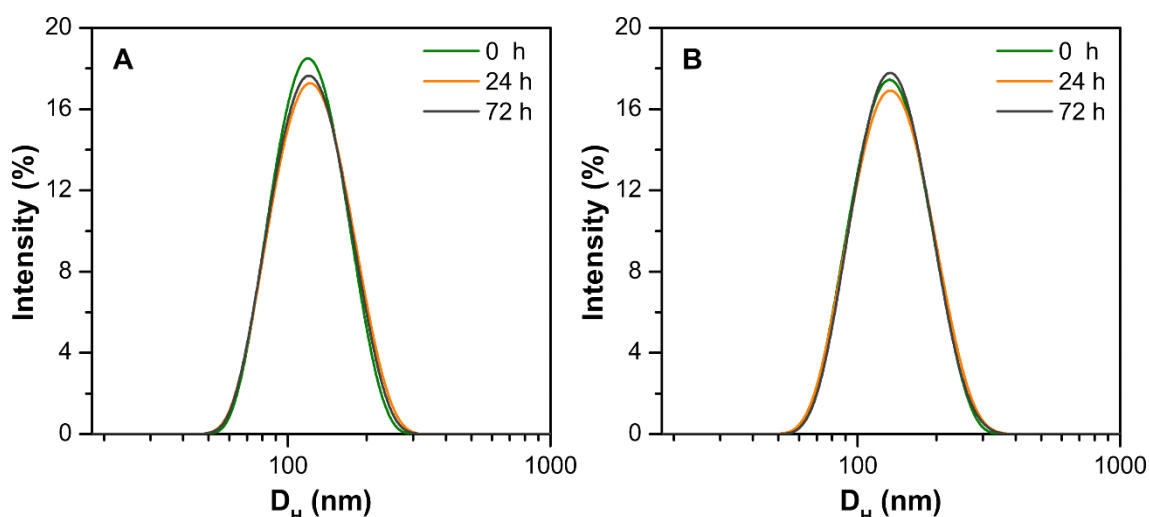


Figure S3. DLS-based size distribution obtained for SNP-FD_{BSA1%} resuspended in PBS at 25°C (A) and DMEM supplemented with 10% of FBS at 37°C (B) after 0h, 24h and 72h of incubation.

Complementary, the impact of storage was studied for SNP-FD_{BSA1%}. After freeze-drying, the lyophilizates were stored at room temperature for selected periods of time and then resuspended in PBS and their size distributions were evaluated by DLS. The DLS-based size distribution obtained for SNP-FD_{BSA1%} is almost unaltered during storage of the powders for up to 6 months (Figure S4).

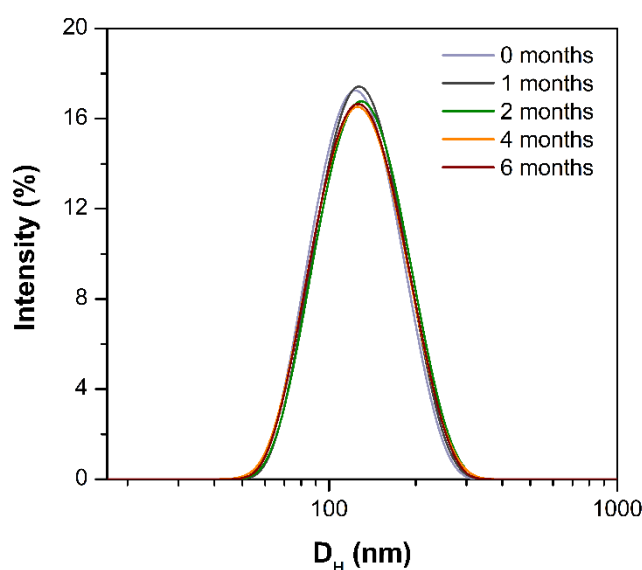


Figure S4. DLS-based size distribution obtained for SNP-FD_{BSA1%} resuspended in PBS at 25°C, after the powders being stored for 0, 1, 2, 4 and 6 months.

Section S7: STEM of SNP-FD_{BSA1%} after freeze-drying

The main SNP used along this work was characterized by STEM after freeze-drying with BSA (1% w/v) and resuspension in water. The idea was to investigate structural features of the resuspended sample without any further alteration. Then, no further purification was done to remove the excess of non-bound BSA. STEM measurements were performed as explained in section S1.

Figure S5 presents the obtained results. As observed in figures S5A and S5B, SNPs appear slightly agglomerated (because they were dried over the TEM grid) but not in intimate contact (like the samples that are irreversibly aggregated). They are embedded in a BSA matrix surrounding (protecting) them. In terms of size and shape, they present the same features seen prior freeze-drying: spheroidal shape and, although less accurate (since the edges of the particles are diffuse due to BSA presence), the size analysis ($D_{STEM}=87.8$ nm, $\sigma=9.1\%$) reveals no significant difference with respect to SNP prior freeze-drying.

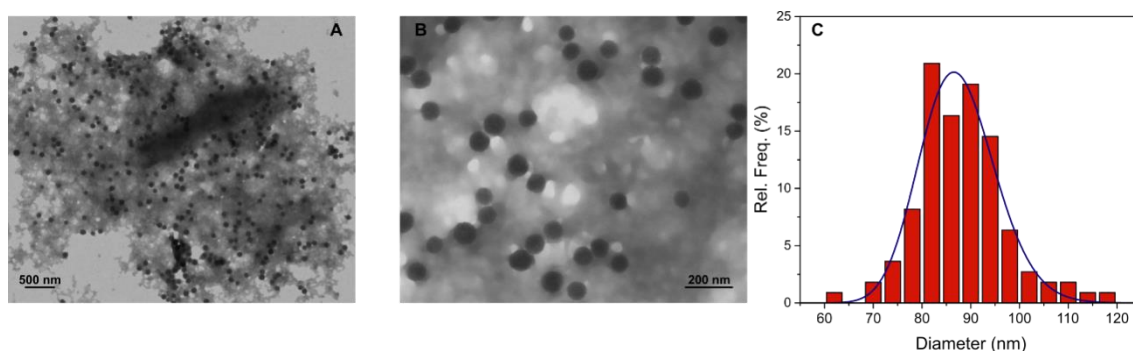


Figure S5. (A and B) Representative STEM images of SNP-FD_{BSA1%} after resuspension. (C) STEM-based size distribution of this sample.

Section S8: Evaluation of Dh_2/Dh_1 for SNP freeze-dried in presence of increasing concentrations of BSA

Figure S6 (orange dots) show the evolution of the ratio between the hydrodynamic diameters obtained after resuspension (Dh_2) in PBS and prior freeze-drying (Dh_1). Dh_2/Dh_1 suffers a seemingly exponential decay with increasing protein concentration. Dh_2/Dh_1 assumes values which are far from 1 in absence or at low BSA concentrations, evidencing strong aggregation. From 0.6% w/v BSA onwards, the ratio reaches a minimum with values between 1.05 and 1.1. We identify this region as the one where the maximum protection efficiency takes place.

In addition, resuspension in water (green dots in Figure S6) of SNP protected with different concentrations of BSA was studied and the results compared to the ones obtained in PBS. The trends are very similar in both media and only minor differences are seen at low BSA contents. This difference may be attributed to the higher PBS ionic strength if compared to water.

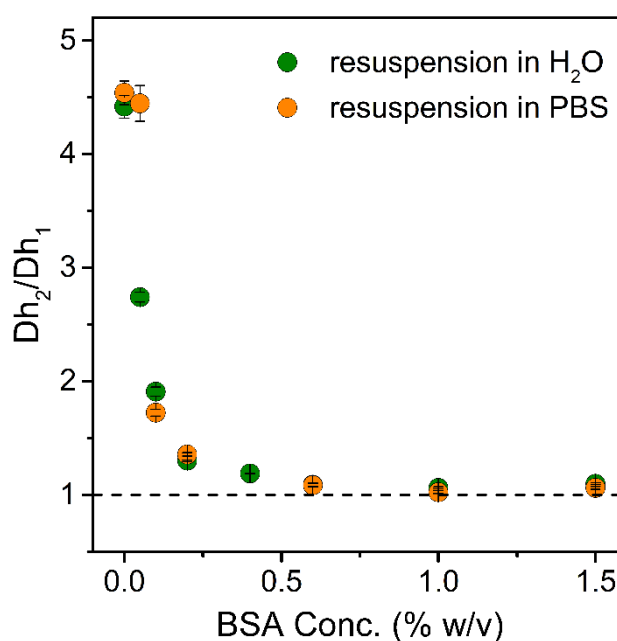


Figure S6. Evolution of SNP's Dh_2/Dh_1 in water (green dots) and PBS (orange dots) with increasing concentration of BSA. Dh_2 and Dh_1 are Dh after and prior freeze-drying, respectively.

Section S9: TGA of SNP after incubation with different BSA concentrations

In order to investigate the amount of strongly adsorbed BSA over SNPs prior freeze-drying, thermogravimetric analysis (TGA) was performed. SNPs were incubated with increasing BSA concentrations and thoroughly washed (by cycles of centrifugation and resuspension as explained in the main manuscript) to remove non-bonded BSA. Three representative BSA concentrations were selected for this experiment: 0.2% w/v (below BSA saturation concentration as indicated by DLS) and 0.6 and 1.0% w/v (above BSA saturation concentration).

TGA experiments were made using a Perkin-Elmer Pyris 1 TGA thermogravimetric analyzer, under N₂ flow. First the samples were pre-heated at 110°C for 20 min to remove adsorbed water.⁸ Then, the temperature was ramped to 850°C at a rate of 5°C/min.

Figure S7A shows the thermograms of bare SNPs and SNPs incubated with 0.2, 0.6 and 1.0% w/v of BSA. The thermograms of SNPs incubated with BSA were compared to the one obtained for bare SNPs to determine mass fractions corresponding to adsorbed BSA. TGA curves of bare SNPs exhibit a weight loss around 5% in the range between 180 and 800°C that is usually attributed to the surface dehydroxylation as well as the complete decomposition and carbonization of the partially or unreacted TEOS remaining in the material.^{9,10} SNPs incubated with different BSA concentrations show larger weight losses in the same range due to the adsorbed protein. Then, it is possible to roughly estimate the fraction of BSA adsorbed (see figure S7B) over SNPs in 6% w/w (for SNPs incubated with 0.2% w/v of BSA), 8.4% w/w (for SNPs incubated with 0.6% w/v of BSA) and 8.6% w/w (for SNPs incubated with 1.0% w/v of BSA) by subtracting the weight loss observed for the bare SNPs from these thermograms in the protein presence.

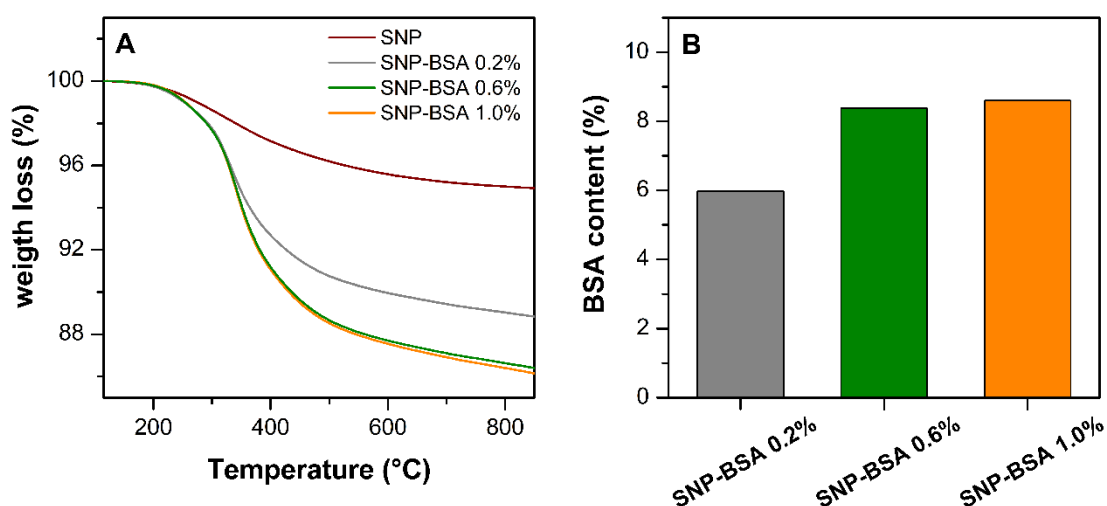


Figure S7. (A) TGA profiles of bare SNPs and SNPs incubated with increasing concentrations of BSA. (B) Estimated BSA adsorbed content on SNPs incubated with increasing concentrations of the protein.

Section S10: Theoretical estimation of the mass fraction corresponding to a BSA monolayer

It is possible to estimate the mass fraction corresponding to a monolayer of BSA over a nanoparticle using simple geometrical considerations. Considering the SNP diameter obtained by STEM ($D_{STEM} = 89.0\text{nm}$), its geometrical specific surface area (SSA_{geo}) can be estimated as:

$$SSA_{geo} = \frac{6000}{D_{STEM} \times \rho_{SNP}}$$

For silica nanoparticles obtained by Stöber procedure, their density is $\rho_{SNP} \sim 1.9\text{ g/cm}^3$.^{11,12} So, for SNP of 89.0 nm its $SSA_{geo} \sim 35.5\text{ m}^2/\text{g}$.

BSA has been modeled as an ellipsoid with dimensions of 14 x 4 x 4 nm.¹³ Assuming that the protein monolayer is formed by BSA molecules with "side-on" orientation (protein largest axis oriented parallel to nanoparticle surface), the area occupied by 1 BSA molecule (A_{BSA}) is estimated by the area of an (projected) ellipse of 14 x 4 nm ($A_{ellipse} = \pi \times a/2 \times b/2$) $\sim 44\text{ nm}^2$ or $4.4 \times 10^{-17}\text{ m}^2$. Then, the amount of BSA adsorbed (BSA_{ads}) per gram of SNPs can be estimated as:

$$BSA_{ads} = \frac{SSA_{geo} \times MW_{BSA}}{A_{BSA} \times N_a}$$

where MW_{BSA} is the molecular weight of BSA ($\sim 66500\text{ Da}$) and N_a is Avogadro's number. By replacing with their respective values (using proper unit conversion), an amount of $BSA_{ads} \sim 0.089\text{ gBSA / gSNPs}$ is obtained.

Finally, the percentual mass fraction of BSA (%BSA) in the complex formed by SNPs and a monolayer of the protein can be estimated as:

$$\%BSA = \frac{BSA_{ads}}{1 + BSA_{ads}} \times 100$$

Using the former equation, 8.2% w/w of BSA is obtained which fairly agrees with the values determined by TGA (in the saturation regime, $\sim 8.5\%$, see Section S9).

Section S11: TGA of SNP-FD_{BSA1%} after freeze-drying and washing

Thermogravimetric analysis (TGA) was performed to investigate the amount of strongly adsorbed BSA over SNP after freeze-drying. SNPs were incubated with BSA 1.0% w/v, submitted to freeze-drying, resuspended in water and then thoroughly washed (by cycles of centrifugation and resuspension as explained in the manuscript) to remove non-bonded BSA. TGA experiments were made using a Perkin-Elmer Pyris 1 TGA thermogravimetric analyzer, under N₂ flow. The samples were pre-heated at 110°C for 20 min to remove adsorbed water.⁸ Then, the temperature was ramped to 850°C at a rate of 5°C/min.

Figure S8 shows the thermograms of bare SNPs and SNPs incubated with 1.0% w/v BSA, before and after freeze-drying (FD). The thermograms of SNPs incubated with BSA were compared to the one obtained for bare SNP to determine mass fractions corresponding to adsorbed BSA. TGA curves of bare SNP exhibit a weight loss around 5% in the range between 180 and 800°C that is usually attributed to the surface dehydroxylation as well as the complete decomposition and carbonization of the partially or unreacted TEOS remaining in the material.^{9,10} The fraction of adsorbed BSA over SNPs can be estimated as 8.6% w/w for SNPs incubated with 1.0% w/v BSA before freeze-drying and 13.6% w/w after freeze-drying by subtracting the weight loss observed for the bare SNP in the same range. This value corresponds to a 5% w/w increase from the value prior freeze-drying and likely indicates that additional protein is adsorbed during freeze-drying over the BSA monolayer.

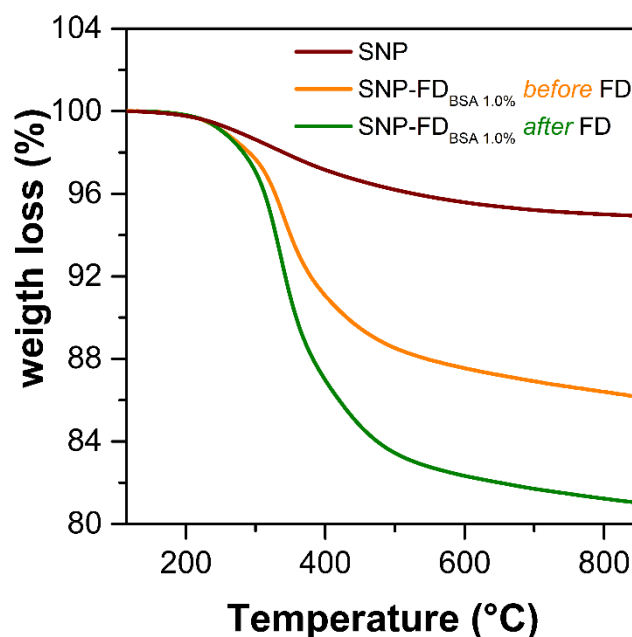


Figure S8. TGA profiles of bare SNPs and SNPs incubated BSA 1.0%w/v before and after freeze-drying.

Section S12: Brief exploration on the freeze-drying of SNPs with different sizes

Two other SNPs sizes were synthesized following the same methodology described in the main text, only varying the amount of ammonia solution added during the synthesis as described before.¹⁴ Figure S9 presents DLS data and STEM images (inset) obtained for these nanoparticles. These nanoparticles exhibited Dh of 165 and 44.6 nm (D_{STEM} around 155 and 40 nm, respectively). STEM was only used to verify size and shape of these particles.

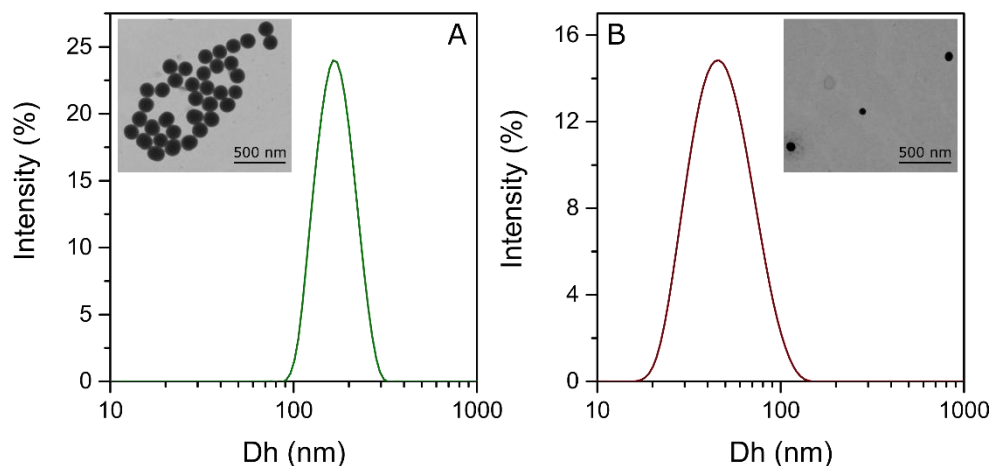


Figure S9. DLS-based size distribution of SNPs with mean Dh's of (A) 165 nm and (B) 44.6 nm, respectively. The insets are representative STEM images of each SNP.

The evolution of nanoparticles Dh and the ratio Dh_2/Dh_1 was followed by increasing BSA concentration (using the same SNP concentration, 1g/L) and the results were compared to those obtained for the original SNP used along this work ($Dh = 106$ nm). Figure S10 shows that the larger SNP (orange dots) seems to be saturated at lower BSA concentrations (around 0.1-0.2 % w/v) when compared to the original SNP (red dots). The maximum protection for SNP of $Dh = 165$ nm against freeze-drying induced aggregation is also attained from 0.2% w/v of BSA onward. Above this concentration the Dh_2/Dh_1 ratio reaches nearly constant values around 1.05-1.1.

It was not possible to precisely follow the BSA adsorption over SNP of $Dh = 44.6$ nm by DLS. The scattering from SNP of $Dh = 44.6$ nm is not as intense as for other SNPs studied in this work (the scattering intensity scales as $I \propto r^6$). Consequently the scattering from BSA contributes considerably to the DLS signal and interferes in the proper Dh determination (SNP + BSA layer). This fact explains the Dh reduction for SNP of $Dh = 44.6$ nm at BSA concentrations above 0.6% w/v. Although it is not possible to accurately determine the BSA concentration required to reach saturation with BSA, the evolution of Dh_2/Dh_1 for SNP of $Dh = 44.6$ nm also follows a seemingly exponential decay. The maximum protection is shifted towards higher BSA concentrations, as expected. In this case, BSA concentrations above 1.5-2.0% w/v were required to reach 1.05-1.1 values for Dh_2/Dh_1 as previously explained.

Furthermore, it is possible to estimate the quantity of BSA required to form a monolayer over both particles ($Dh_{44.6}$ and 165nm) based on their geometrical SSAs (20.4 and 78.9 m^2/g , respectively) as explained in Section S10. For the largest SNP, an

amount of 0.051 g of BSA per gram of SNP is required to form a BSA monolayer, while the smaller one would require 0.196 g per gram of SNP. If at 0.6 % w/v (6 g/L) of BSA the three nanoparticles were saturated with BSA (just for illustration purposes), the quantity of free BSA can be calculated after subtraction of the adsorbed BSA from the total BSA amount. As such, for SNP of $D_h = 165$ nm, the free BSA amount would be estimated 5.95 g/L, while for SNP of $D_h = 106$ nm and SNP of $D_h = 44.6$ nm, free BSA concentrations would be 5.91 g/L and 5.80 g/L, respectively. Despite the amount of adsorbed BSA being different for all nanoparticles, the free BSA concentration (which would be the main contribution to the vitrification properties) is similar among all SNP used. Therefore, we can assume that, if vitrification were the only protection mechanism against the detrimental effects of freeze-drying, then the minimum BSA concentration required to successfully protect SNP of different sizes would be similar.

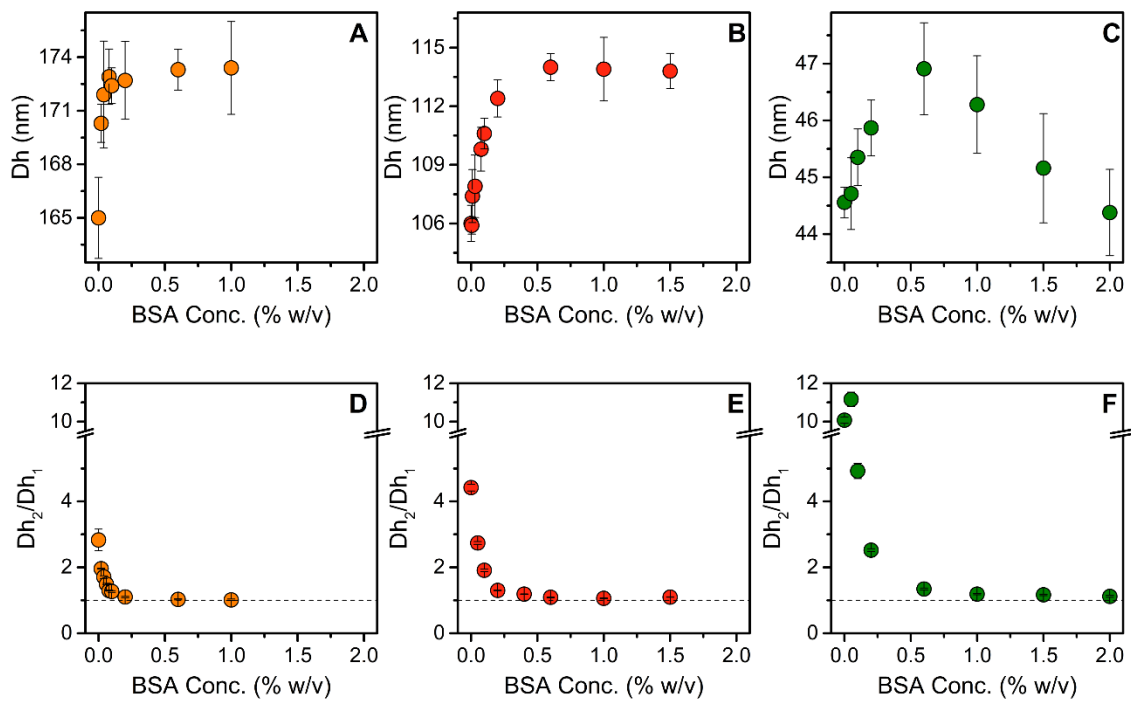


Figure S10. Hydrodynamic diameters of SNP in water with increasing BSA concentration for different SNP (A) 165 nm, (B) 106 nm and (C) 45 nm. Evolution of SNP's D_{h_2}/D_{h_1} with increasing BSA concentration for different SNP: (D) 165 nm, (E) 106 nm and (F) 45 nm. D_{h_1} and D_{h_2} represent the D_h prior and after freeze-drying, respectively.

Section S13: Raw optical density data from hemolytic activity assay

Figure S11A shows the raw optical density (O.D.) data measured at 540 nm in the hemolytic assays (supernatants) of SNP-FD at different concentrations (red points; between red parenthesis are presented the obtained values for %hemolysis calculated using the corresponding negative and positive controls). In addition, Figure S11A also shows the raw O.D. data obtained for non-freeze-dried SNPs (non-FD) from a different batch with similar nanoparticle size (grey points) in the concentration range of 100-1000 mg/L. Above 100 mg/L SNP-non-FD produce less hemolysis (maximum of 41% at 500 mg/L) than SNP-FD. These differences in the hemolytic behavior may be attributed to the presence of aggregates^{15,16} (SNP-FD exhibits aggregates in suspension, as seen by DLS, while non-SNP-FD does not) and/or the minor impact that the freeze-drying process might have on the nanoparticle surface properties.

Figure S11 B and C show raw O.D data obtained in the cases of SNP-FD_{BSA} (protected with 0.2, 0.6 and 1.0 % of BSA) at 100 mg/L (Figure S11B) and 800 mg/L (Figure S11C). O.D. data from protected SNP-FD_{BSA} (both nanoparticle concentrations and all BSA concentrations) is nearly the same to the one observed for the negative control (C-). Consequently, the calculated % of hemolysis (as explained in Section S2) for SNP-FD_{BSA} samples is close to zero in all cases.

Finally, Figure S11D shows the raw O.D. from hemolysis tests of non-freeze-dried SNP (at 800 mg/L) incubated with 0.6 and 1% of BSA and of washed SNP-FD_{BSA} (at 800 mg/L, protected with 0.6 and 1% of BSA). All conditions presented O.D. similar to C-.

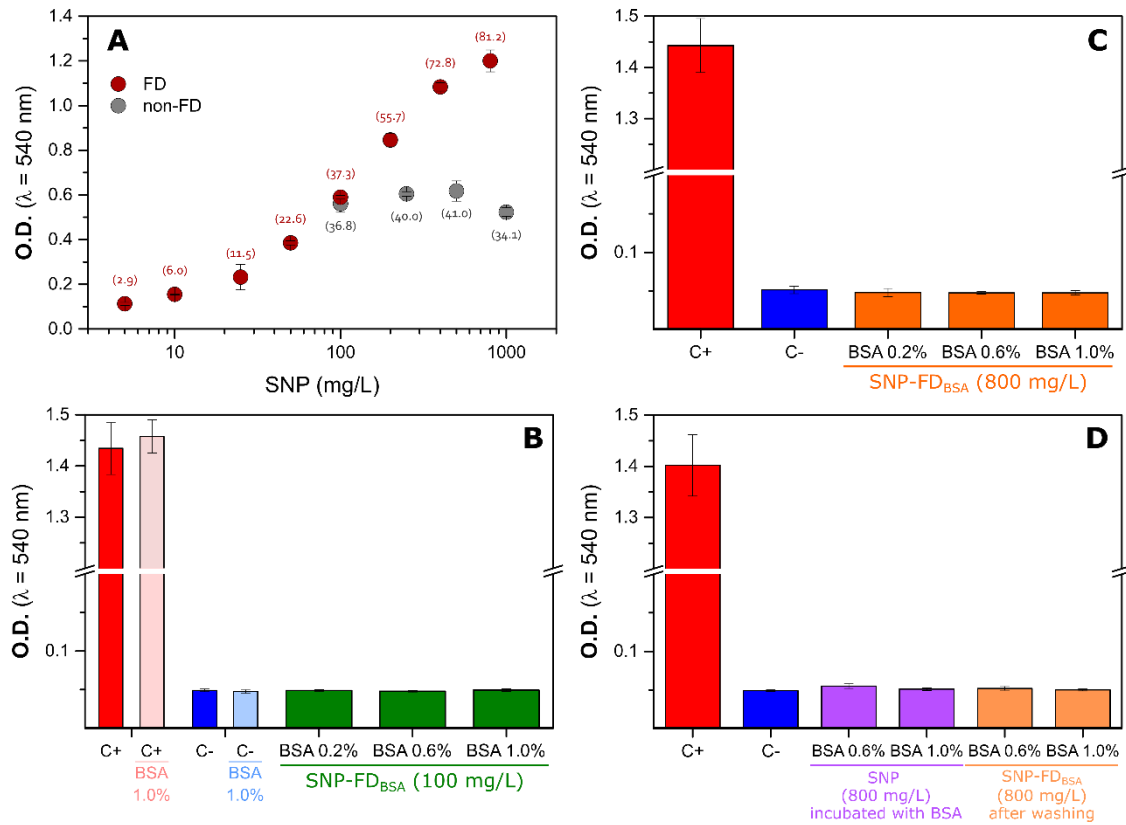


Figure S11. (A) Optical density (O.D.) values (at 540 nm) measured during the hemolytic assays (supernatants) of SNP-FD (red points) and SNP-non-FD (grey points). The values of % hemolysis calculated for each OD (using the corresponding negative and positive controls) are presented between parenthesis (using the same color code). (B), (C) and (D) present the O.D. values obtained for SNP-FD_{BSA} at 100 mg/L (B), SNP-FD_{BSA} at 800 mg/L (C) and SNPs incubated with BSA and SNP-FD_{BSA} washed after freeze-drying and resuspension (D). C+ and C- mean positive and negative control, respectively.

Section S14: Brief exploration on the use of other proteins than BSA as protectants for the freeze-drying of SNPs

The use of human serum albumin (HSA, Mw = 66.4 KDa) and β -lactoglobulin from bovine milk (BLG, Mw = 18.2 KDa) as protectants during freeze-drying was investigated. Both proteins were purchased from Sigma-Aldrich. The characterization prior and after freeze-drying of nanoparticles were performed following the same procedure used for the testing of BSA as protectant. Silica nanoparticles of Dh ~ 118 nm were used.

Roughly, the adsorption of HSA over SNP (at 1g/L) produce a corona of around 8 nm (like BSA) at saturation (Figure S12A). Qualitatively, the interaction seems to be weaker than that observed for BSA. The increment in size with increasing protein concentration seems not to be as steep as those observed for BSA, and the saturation apparently is reached at higher concentration compared to the latter. Moreover, considering that the particle used in these tests is larger than that used with BSA, if the interaction between HSA and the nanoparticle surface were similar to that observed for BSA, the saturation should be attained at a lower protein concentration. After freeze-drying and resuspension (in PBS at 1g/L, as explained for BSA) the SNPs seems to reach similar sizes to that observed prior freeze-drying (i.e. $Dh_2/Dh_1 \sim 1$; where Dh_2 and Dh_1 are the Dh measured after and prior freeze-drying, respectively) when HSA is used above 0.8 - 1 %w/v (Figure S12C). In addition, differently from BSA, no protection at all is observed at low HSA concentrations, where the resuspension quality is comparable or even worst to the non-protected SNP.

The effectiveness of BLG as protectant was explored in less detail (less concentrations were used) than HSA and BSA. Roughly, BLG seems to form a corona of around 5 – 6 nm around SNP (Figure S12B). This is expected given the lower BLG molecular weight compared to BSA and HSA. BLG seems to protect SNP from freeze-drying induced aggregation from 0.6 % w/v onwards (Dh_2/Dh_1 close to 1; Figure 12D). In addition, a relatively good level of protection is observed at low concentrations.

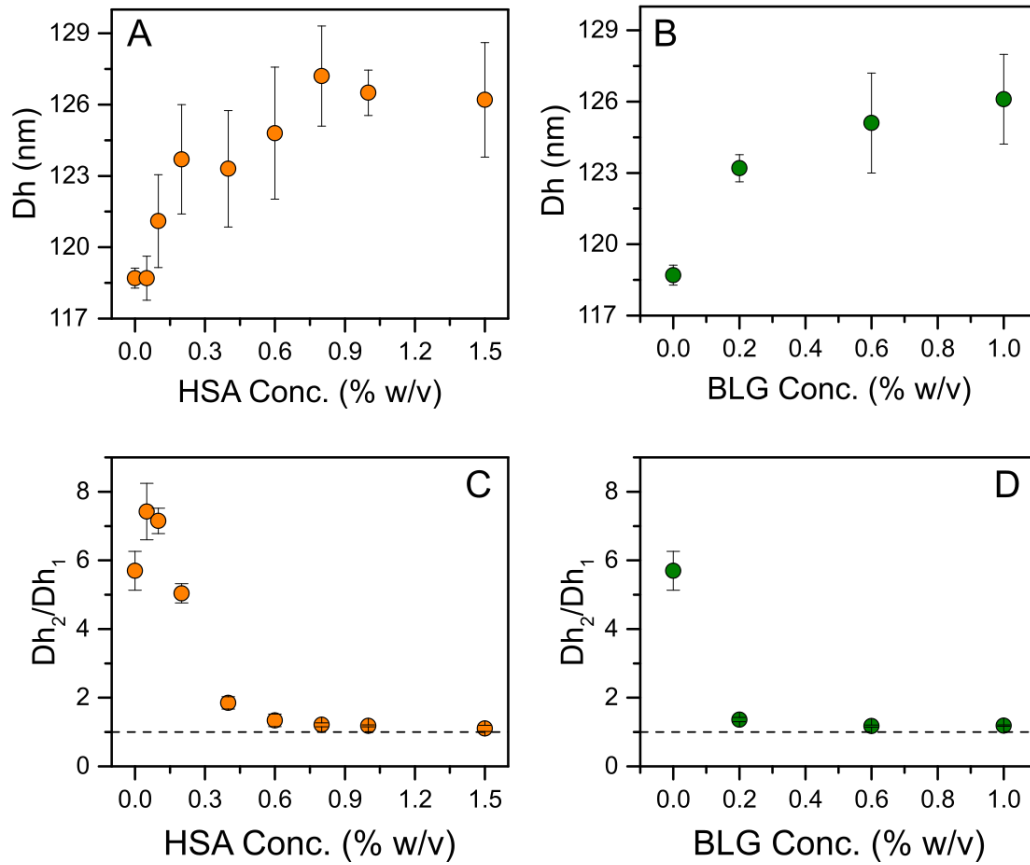


Figure S12. Evolution of SNP Dh with increasing concentrations of (A) HSA and (B) BLG. Evolution of the ratio between the Dh after (Dh₂) and prior (Dh₁) freeze-drying with increasing concentrations of (C) HSA and (D) BLG.

Section S15: Impact of washing on the DLS-based size of SNPs incubated with 1% w/v BSA

The impact of washing on the size of SNP incubated with 1% w/v BSA was investigated by DLS. DLS measurements were performed prior and after washing. Washing was performed by cycles of centrifugation and resuspension as explained in the main manuscript and Figure S13 shows the results. The size observed by DLS is increased after washing (from ~ 114 nm to 121 nm). This increment can be attributed to the washing procedure (several centrifugation steps) which may induce some subtle agglomeration or aggregation.¹⁷ Based on this result, we understand that is not accurate to estimate the BSA corona thickness by DLS after washing.

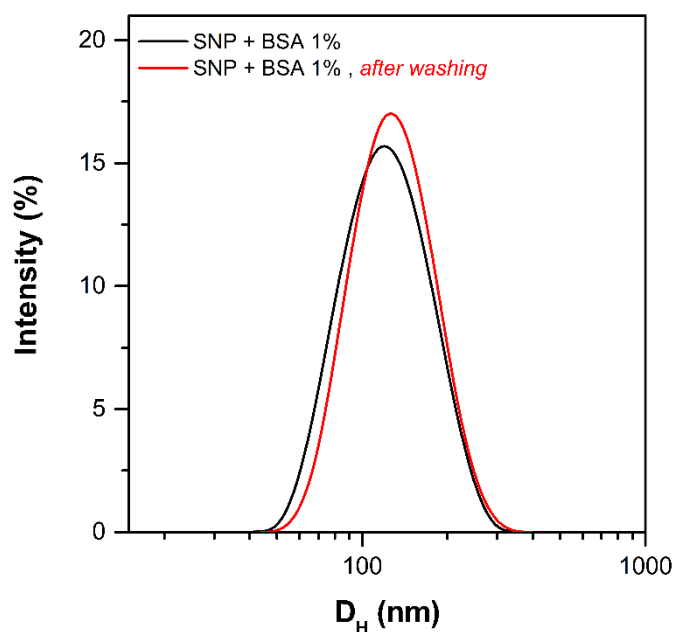


Figure S13. DLS-based size distribution of SNP + BSA 1% w/v. obtained prior and after washing.

SECTION S16: Brief evaluation on freeze-drying of SNP with freezing step carried at higher temperature

The impact of the freezing temperature in the protection exerted by BSA during freeze-drying was preliminary studied for SNP and SNP+BSA 1%. The freezing step was carried in a freezer working at temperatures below -30°C for 24h. Then the sample was placed in the freeze-drier apparatus and resuspended as described in the main manuscript (Experimental - Freeze-drying of SNPs and Resuspension experiments). DLS-based size distributions are shown in Figure S14. Similar results to those observed when SNP-FD_{BSA1%} was freeze-dried using liquid nitrogen to freeze the sample.

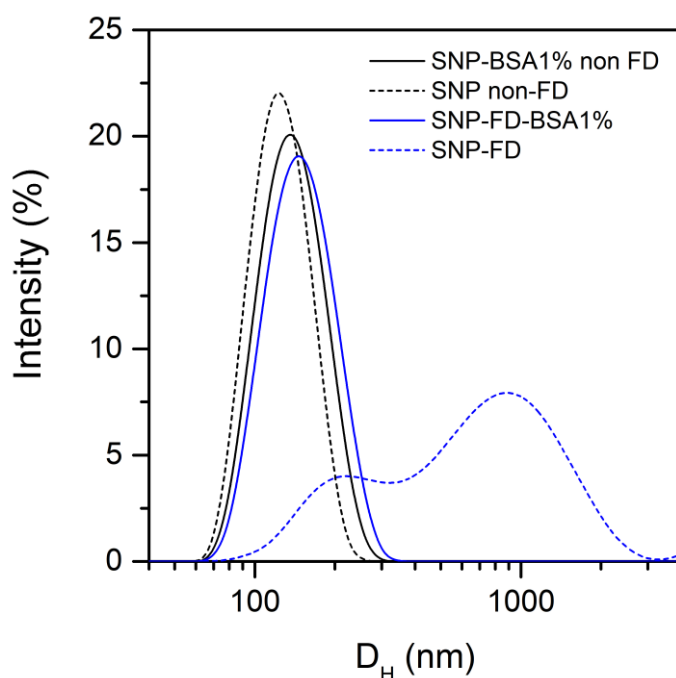


Figure S14. DLS-based size distribution obtained for SNP (dashed lines) and SNP+BSA 1% (solid lines), before (black) and after (blue) freeze-drying with freezing step carried at -20°C .

SECTION S17: Impact of sonication in SNP-FD

Sonication was performed (using an Eco-Sonic Q3.0L equipment from Ultrasonic or an USC 800 equipment from Unique) to evaluate if the aggregation observed for SNP-FD was reversible by applying a harsher homogenization method than just vial mixing. DLS-based size distributions are shown in Figure S15.

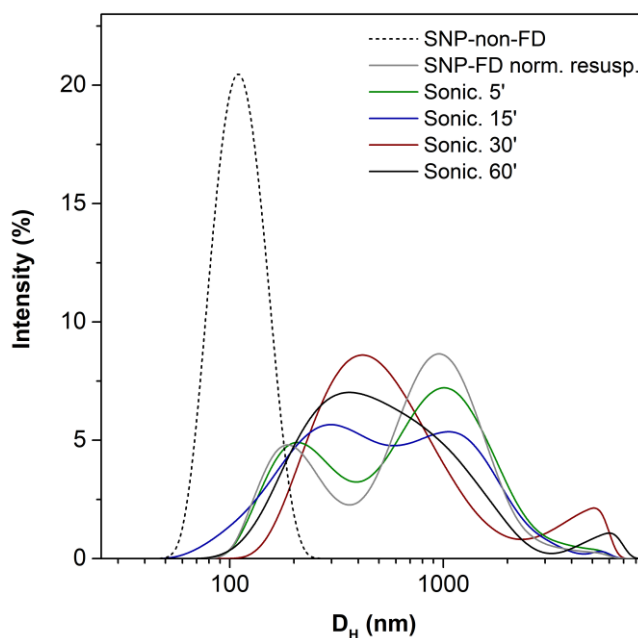


Figure S15. DLS-based size distribution obtained for SNP-non-FD, SNP-FD resuspended by gently mixing (norm. resusp) and with sonication for 5, 15, 30 and 60 min.

Section S18: References

- 1 C. A. Schneider, W. S. Rasband and K. W. Eliceiri, *Nat. Methods*, 2012, **9**, 671–675.
- 2 O. Glatter and O. Kratky, *Small Angle X-Ray Scattering*, Academic Press, 1982.
- 3 I. Breßler, J. Kohlbrecher and A. F. Thünemann, *J. Appl. Crystallogr.*, 2015, **48**, 1587–1598.
- 4 W. Schärtl, *Light Scattering from Polymer Solutions and Nanoparticle Dispersions*, Springer, Heidelberg, 2007.
- 5 R. Curvale, M. Masuelli and A. P. Padilla, *Int. J. Biol. Macromol.*, 2008, **42**, 133–137.
- 6 R. Pamies, J. G. Hernández Cifre, M. del Carmen López Martínez and J. García de la Torre, *Colloid Polym. Sci.*, 2008, **286**, 1223–1231.
- 7 V. Ball and J. J. Ramsden, *Biopolymers*, 1998, **46**, 489–492.
- 8 Z. G. Estephan, J. A. Jaber and J. B. Schlenoff, *Langmuir*, 2010, **26**, 16884–16889.
- 9 S. Li, Q. Wan, Z. Qin, Y. Fu and Y. Gu, *Langmuir*, 2015, **31**, 824–832.
- 10 M. B. de Oliveira, L. F.; Goncalves, K. d. A.; Boreli, F. H.; Kobarg, J.; Cardoso, J. *Mater. Chem.*, 2012, **22**, 22851–22858.
- 11 A. Labrosse and A. Burneau, *J. Non. Cryst. Solids*, 1997, **221**, 107–124.
- 12 Q. Wan, C. Ramsey and G. Baran, *J. Therm. Anal. Calorim.*, 2010, **99**, 237–243.
- 13 T. Peters, *All about albumin : biochemistry, genetics, and medical applications*, Academic Press, 1996.
- 14 A. S. Picco, L. F. Ferreira, M. S. Liberato, G. B. Mondo and M. B. Cardoso, *Nanomedicine*, 2018, **13**, 179–190.
- 15 L. C. J. Thomassen, V. Rabolli, K. Masschaele, G. Alberto, M. Tomatis, M. Ghiazza, F. Turci, E. Breynaert, G. Martra, C. E. A. Kirschhock, J. A. Martens, D. Lison and B. Fubini, *Chem. Res. Toxicol.*, 2011, **24**, 1869–1875.
- 16 C. Pavan, M. Tomatis, M. Ghiazza, V. Rabolli, V. Bolis, D. Lison and B. Fubini, *Chem. Res. Toxicol.*, 2013, **26**, 1188–1198.
- 17 M. Pálmai, L. N. Nagy, J. Mihály, Z. Varga, G. Tárkányi, R. Mizsei, I. C. Szigyártó, T. Kiss, T. Kremmer and A. Bóta, *J. Colloid Interface Sci.*, 2013, **390**, 34–40.
- 18 S. M. Patel, S. L. Nail, M. J. Pikal, R. Geidobler, G. Winter, A. Hawe, J. Davagnino and S. Rambhatla Gupta, *J. Pharm. Sci.*, 2017, **106**, 1706–1721.